

# LAYOUT OF THE UPGRADED HERA INTERACTION REGIONS

M. Seidel, F. Willeke

Deutsches Elektronen Synchrotron DESY, Notkestr. 85, 22603 Hamburg

## Abstract

DESY pursues a luminosity upgrade project [1] for the HERA electron proton collider with the goal to raise the luminosity by a factor 5 compared to original design parameters. The major part of this increase is achieved by installing new interaction regions in 2000/2001. The new scheme involves a very early separation of the colliding beams by means of superconducting magnets that are installed inside the experimental detectors. The early beam separation allows to position the final focus quadrupoles closer to the IP, which in turn leads to smaller beam spot-sizes and higher luminosity.

The beam separation inside the detectors causes two major problems. About 28kW of synchrotron radiation power is produced in the separation magnets, i.e. in the detectors. Secondly the strong bending magnets tend to deflect low energy electrons, produced by beam-gas bremsstrahlung interactions, onto the detector beampipe. Both effects present qualitatively new background sources for the detectors. We describe how these problems are counteracted with the specifically adopted layout of the geometry and the vacuum system in the new interaction regions.

## 1 OVERVIEW

The new HERA interaction region (IR) is layed out to allow collisions of 920 GeV Protons with 30 GeV electrons. At startup the electron machine will run at 27.5 GeV, an energy which is more preferable in view of a high degree of beam polarization. The most important beam parameters are listed in table 1.

	e-Beam	p-Beam
energy [GeV]	27.5	920
beam current [mA]	58	140
emittance [nm]	20	5000/ $\gamma$
emittance ratio $\varepsilon_y/\varepsilon_x$	0.17	1
rms b. length [mm]	10	191
beta-funcs. $\beta_x^*, \beta_y^*$ [m]	0.63, 0.26	2.45, 0.18
b. size $\sigma_x \times \sigma_y$ [ $\mu\text{m}^2$ ]	$112 \times 30$	$112 \times 30$
bb tune shift/IP $\Delta\nu_{x,y}$	0.033, 0.051	0.0014, 0.0004
minimum aperture [ $\sigma$ ]	20	12
Luminosity	$7.5 \cdot 10^{31} \text{cm}^{-2} \text{s}^{-1}$	

Table 1: Start-up parameters for the HERA upgrade.

In order to separate the beams two superconducting combined function magnets will be installed inside the experimental detectors, about 2 m from the interaction point (IP).

The early beam separation allows to position the focusing quadrupoles for the proton beam much closer to the IP, which in turn allows to reduce the spot size. The electron beam will be focused stronger as well and in addition its emittance will be reduced by increasing the betatron phase advance in the arcs from  $60^\circ$  to  $72^\circ$  [2]. The cross sections of the two beams are exactly matched at the IP in order to avoid intolerable beam-beam effects. The interaction region allows also to collide positrons with protons. In this case the separation magnets have to switch polarity which disturbs the trajectory and optics of the proton beam. While the optics error can be corrected by changing quadrupole currents, the trajectory error has to be compensated by shifting the IP 7.5 mm towards the ring center and also moving 5 quadrupoles by a few mm. Any other, more convenient solution for switching the lepton species, would require an additional bending magnet at the expense of increasing the distance of the quadrupoles to the IP, and consequently the loss of luminosity.

The electron beam produces a significant amount of synchrotron radiation (SR) within the superconducting (sc.) separation magnets. In order to allow for safe passage of this SR the sc. magnet on the downstream side of the IP needs a larger aperture and a shorter length than the one on the upstream side. To obtain the same focusing strength we have added a normalconducting quadrupole on the downstream side. Consequently the new IR is not exactly symmetric which introduces some difficulties especially for spin matching of the electron lattice. To realize the new concept, the whole IR, up to about 65 m distance from the interaction point, has to be modified. New magnets were designed and manufactured. The design of each magnet has been adopted to the special requirements at its location, as for example beam envelopes, the distance to the other beam, or the need to safely handle SR. In parallel to the luminosity upgrade both *ep* IR's will be equipped with spin rotators [3] that turn the spin orientation from transverse to longitudinal direction over the IR. A schematic overview of the inner part of the IR is shown in Fig. 1.

## 2 PARTICLE BACKGROUND

The major qualitative change in the IR layout is the early beam separation in the detectors, very close to the IP's. Electrons that have lost energy due to beam gas interactions upstream of the IR will preferentially hit the detector beampipe because they receive a larger deflection angle by the separation fields. In order to relax this problem we have foreseen to install a dispersive magnet structure, called "dogleg", in the straight section upstream of the detector, and for symmetry reasons also downstream. The

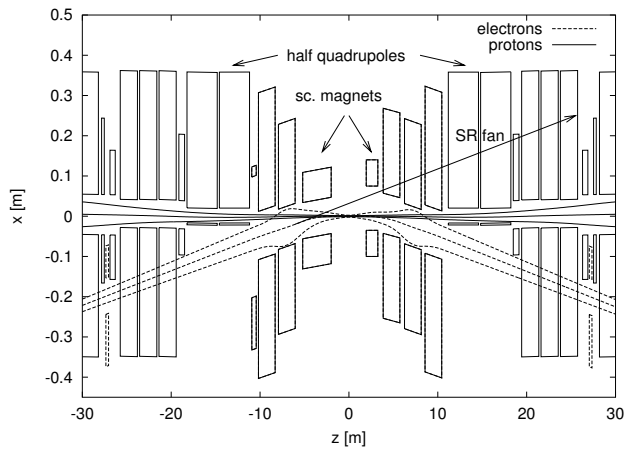


Figure 1: Top view schematic layout of the interaction region.  $20\sigma_x$  beam envelopes are indicated for the electrons and  $12\sigma_x$  for the protons.

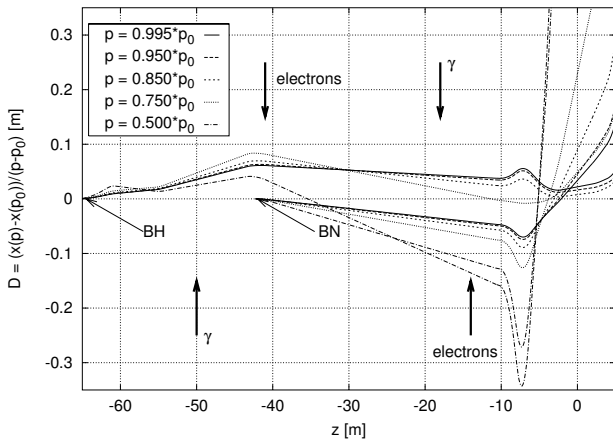


Figure 2: Dispersion orbits, normalized to momentum deviation, for particles that undergo bremsstrahlung events upstream of the dogleg and in-between the magnets. The positions of photon and particle collimators are indicated.

purpose of the dogleg is to separate low energy particles from the beam and to allow for momentum collimation. The dogleg contains two dipole magnets that deflect the beam back and forth. Dispersion functions for off-energy particles produced in different regions are shown in Fig. 2. Movable particle collimators are foreseen at -42 m and -14 m distance to the IP. Tracking simulations were performed to estimate the efficiency of the momentum collimation [4]. With particle collimators at distances from the beam of about  $9\sigma_x$  nearly all bremsstrahlung-electrons generated beyond -40 m, that would otherwise hit the detector beam pipe, are removed. For the remaining straight section in the IR we try to improve the residual gas pressure.

The dogleg bending magnets produce significant amounts of SR, 1.6 kW and 1 kW. In order to shield the detector beam pipe from this radiation, movable collimators are installed at -50 m and -19 m in addition.

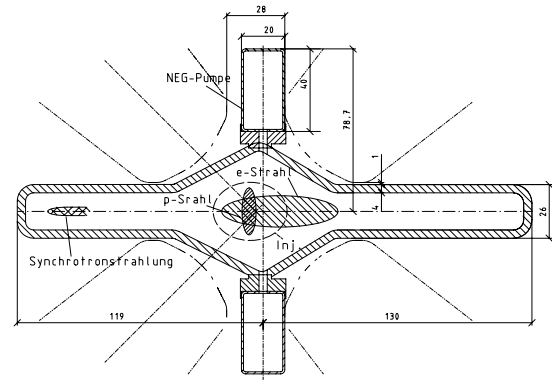


Figure 3: Cross section of the electron-downstream vacuum chamber in the first triplet magnet. The left side extension allows transport of the SR-fan.

### 3 SYNCHROTRON RADIATION

The SR produced in the separation magnets and especially in the upstream final focus triplet presents a serious background problem for the detectors. At 30 GeV the total radiation power amounts to 28 kW and relatively hard photons with critical energies of up to 150 keV are produced. Nevertheless the radiation power deposited on the detector beam pipe has to stay well below  $1\mu\text{W}$ . At this level backscattered light from downstream absorbers plays a role as well as possible tails of the electron beam distribution. The radiation from the triplet is not easy to be collimated since a collimator that moves close to the electron beam from the outside would disturb the proton beam (Fig. 1). Only at distances to the IP of less than 5 m, i.e. inside the sc. magnet, such a collimator would become effective. Therefore the beam pipes inside the sc. magnets and the detector have apertures large enough to allow passage of the SR-tail down to the required small intensities. However, since it is possible that non-Gaussian tails of the electron beam produce significantly wider tails in the SR-distribution, there is work under way to design a collimator that reaches about 0.5 m into the sc. magnet. This collimator would allow for direct collimation of the tail photons.

On the electron-downstream side of the detector the SR could not immediately be absorbed since this would result in too much backscattered radiation. Magnets and vacuum chambers (Fig. 3) are laid out such as to allow transport of the radiation fan to a distance of 26 m from the IP, where it is absorbed eventually. Beyond 11 m distance to the IP the common vacuum system is separated into 3 different pipes - one for the proton beam, one for the electrons and one for the outer SR-fan. At the separation point a part of the radiation has to be absorbed on a special high-power absorber [5].

In order to make reliable predictions of the radiation fan, especially in the low density tails, a specific code has been developed that follows a semi-analytic approach. The ra-

diation power per longitudinal slice of a dipole magnet is given by  $dP/dl = 14.1E^4I/\rho^2$ , where  $dP/dl$  is the radiated power in kW/m,  $E$  is the beam energy in GeV,  $I$  the beam current in A and  $\rho$  the bending radius in m. For high energies the intrinsic opening angle of the radiation  $1/\gamma$  is small compared to the beam divergence and one can assume that the photons are radiated exactly along the trajectory of the particle. Consequently the distribution of the photon beam, radiated in a slice of a combined function magnet, is given by:

$$\frac{dp}{dl}(x, x', y, y') = \frac{14.1E^4I}{14.1E^4I [(1/\rho + Kx)^2 + K^2y^2]} f_b(x, x', y, y')$$

Now  $dp/dl$  is the power radiated per unit length of magnet and per unit phase space element.  $K$  is the focusing strength of the magnet in  $m^{-2}$  and  $f_b$  the beam distribution function which we assume to be Gaussian:

$$f_b(x, x', y, y') = \frac{\exp\left(-\frac{I_x(x, x')}{\varepsilon_x}\right) \exp\left(-\frac{I_y(y, y')}{\varepsilon_y}\right)}{4\pi^2 \varepsilon_x \varepsilon_y}$$

$$I_x(x, x') = \frac{\gamma_x x^2 + 2\alpha_x x x' + \beta_x x'^2}{2}$$

Here  $\alpha_{x,y}, \beta_{x,y}, \gamma_{x,y}$  are the beam optical functions,  $\varepsilon_{x,y}$  the beam emittances and  $I_{x,y}$  the action variables for particles.  $I_y$  is defined equivalently to  $I_x$ .

Often one is interested in the power distribution projected onto a certain plane of interest, eg. the beam pipe cross-section at a background sensitive location. For this purpose the above distribution is projected over a certain distance  $\Delta z$  via a simple coordinate transformation:  $x_1 = x_0 + \Delta z x'_0$ ,  $x'_1 = x'_0$ , and equivalently for  $y$ . To obtain the  $x, y$  projection the dependencies on  $x'_1, y'_1$  are integrated out analytically. The above mentioned code steps through the magnet structure and sums up the power contributions from thin magnet slices with their local beam optical functions. Tilt angles of the observation plane against the beam orbit are taken into account. The result is a two (or one-) dimensional power density distribution as depicted in Fig. 4. This location is the exit of the downstream sc. magnet, where the far radiation tail hits the beam pipe and the detector could potentially suffer from backscattered radiation. From the curve one estimates a few  $\mu W$  radiation power on the chamber wall, which is acceptable.

In order to estimate the effect of non-Gaussian tails the above described procedure is carried out with a particle distribution modelled as the sum of two Gaussians, a core distribution and a wider one containing a small fraction of the particles. During dedicated machine studies in 1999/2000 scraper tail scans were carried out at the HERA electron machine [6], with the new  $72^\circ$  optics installed. Scrapers were moved close to the beam from both sides (separately) until the beam lifetime is reduced to a few minutes. In parallel loss monitor rates from shower detectors near the

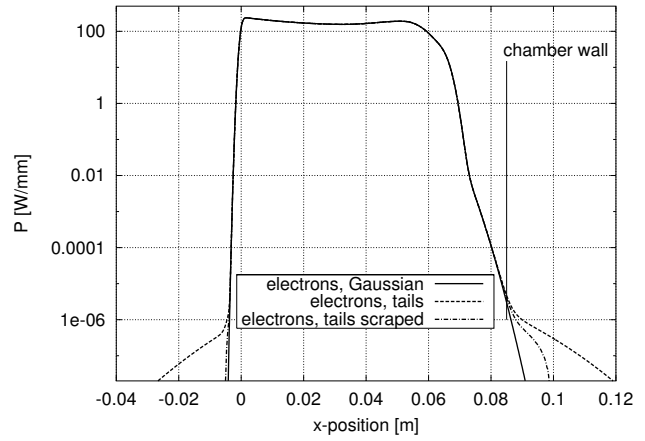


Figure 4: Projected SR line density on a plane perpendicular to the beam at  $z = 3.6$  m, details on the individual curves in the text.

scrapers were observed and recorded. Significantly higher loss rates than predicted from the calculated core emittance are observed for lifetimes of about 10 hours or longer. This means that the real distribution departs from a pure Gaussian for  $x \geq 6.1 \sigma_x$ . If we assume that the second Gaussian has a 3 times wider emittance than the core emittance, we find that a fraction of about  $2 \cdot 10^{-7}$  is contained in the second Gaussian. A noticeable difference in the radiation profile exists only at power densities dropped 8 orders of magnitude below peak power (Fig. 4). The amount of power deposited on the chamber wall would increase only slightly as compared to the case without tails.

Collimation of the particle beam tails at some appropriate location in the machine can help to reduce the SR tails. The dash-dot curve in Fig 4 shows the simulation with tails, and with the beam scraped at  $7.5 \sigma_x$  in addition. The tails are reduced, however, it has to be noted that scraping at this level is practically rather tedious since already small orbit distortions can lead to quick beam losses.

Orbit distortions of the electron beam can also be a cause of intolerable SR background. According to simulation studies this can be kept under control by orbit correction procedures [7].

In summary we are confident that the two major backgrounds, bremsstrahlung electrons and synchrotron radiation, can be controlled satisfactory with the described methods in the new interaction regions.

## 4 REFERENCES

- [1] U. Schneekloth (ed.), DESY-HERA 98-05 (int. report), 1998
- [2] G. Hoffstätter, these proceedings
- [3] J. Buon, K. Steffen, NIM, A245:248, 1986
- [4] the simulations were performed by U. Kötze, DESY, ZEUS
- [5] M. Bieler et al., PAC, New York, 1999
- [6] A. Meseck, in DESY-HERA 00-02 (internal report), 2000
- [7] Ch. Montag, F. Stulle, these proceedings